



Cite this: *RSC Mechanochem.*, 2025, 2, 159

Received 2nd April 2024
Accepted 17th November 2024
DOI: 10.1039/d4mr00028e
rsc.li/RSCMechanochem

Mechanochemical synthesis of rock salt-type $\text{Na}_2\text{CaSnS}_4$ as a sodium-ion conductor[†]

Hamdi Ben Yahia, * Atsushi Sakuda, and Akitoshi Hayashi, *

$\text{Na}_2\text{CaSnS}_4$ was prepared by mechanochemical synthesis from a mixture of Na_2S , CaS , and SnS_2 . The crystal structure was determined from X-ray powder diffraction data. The chemical composition was confirmed by energy dispersive X-ray spectroscopy, and the ionic conductivity was measured using electrochemical impedance spectroscopy. $\text{Na}_2\text{CaSnS}_4$ crystallizes with a rock salt-type structure, space group $Fm\bar{3}m$, $a = 5.6842$ (3) Å, $V = 183.66$ (2) Å³, and $Z = 1$. All the cations are statistically disordered over a unique crystallographic site and are octahedrally coordinated to the sulfur atoms. The ionic conductivity of $\text{Na}_2\text{CaSnS}_4$ is 4.2×10^{-8} S cm⁻¹ ($E_a = 0.6$ eV) at 33 °C.

1. Introduction

Solid electrolytes are materials that exhibit proton, lithium, sodium, potassium, silver, fluoride, or oxide ion conduction. They have been widely used in several all-solid-state electrochemical devices such as gas sensors, capacitors, smart windows, fuel cells, and batteries. In the latter, it is desirable to have a solid electrolyte exhibiting high ionic conductivity in the order of 10^{-2} – 10^{-3} S cm⁻¹ at room temperature to be comparable to liquid electrolytes. Nevertheless, materials with lower ionic conductivities can be implemented in batteries. These solid electrolytes should also be dense with a negligible electronic conductivity and a wide electrochemical stability window.¹

For all solid-state sodium ion batteries (ASSBs), three types of electrolytes are known (*i.e.* polymers, inorganic compounds, and their combinations). Among the crystalline inorganic compounds, one can find oxides, sulfides, and boron hydrides.² Examples thereof are the oxides sodium-beta-alumina $\text{Na}\beta''\text{-Al}_2\text{O}_3$,³ the NASICON-type compounds $\text{Na}_{1+x}\text{Zr}_2\text{Si}_x\text{P}_{3-x}\text{O}_{12}$ ($0 \leq x \leq 3$),⁴ the layered-type compounds $\text{Na}_2\text{M}_2\text{TeO}_6$ ($\text{M} = \text{Ni, Co, Zn, Mg}$),⁵ the sulfides Na_6MS_4 ($\text{M}^{2+} = \text{Mg, Zn}$),⁶ Na_5MS_4 ($\text{M}^{3+} = \text{Al, Ga, In}$),^{7–9} Na_4MS_4 ($\text{M}^{4+} = \text{Si, Ge, Sn}$),^{10–12} Na_3BS_3 ,¹³ Na_3MS_4 ($\text{M}^{5+} = \text{P, As, Sb}$),^{14–16} and Na_2MS_4 ($\text{M}^{6+} = \text{Mo, W}$);^{17,18} and the boron hydrides $\text{Na}_2(\text{CB}_{11}\text{H}_{12})(\text{CB}_9\text{H}_{10})$,¹⁹ $\text{Na}_3\text{BH}_4\text{B}_{12}\text{H}_{12}$,²⁰ or $\text{Na}_4(\text{CB}_{11}\text{H}_{12})_2(\text{B}_{12}\text{H}_{12})$.²¹ The ionic conductivity of these end member materials does not exceed 4×10^{-3} S cm⁻¹ at room temperature. However, in binary systems such as that of

$\text{Na}_3\text{SbS}_4\text{-Na}_2\text{WS}_4$, it can reach up to 10^{-2} S cm⁻¹ at room temperature.²²

The mechanical milling technique has attracted much attention as a procedure for preparing amorphous, crystalline, and composite materials. Indeed, the intensive grinding of particulates, especially through high-energy milling, provides conditions favorable for initiating changes in the particulates. These changes include solid state chemical reactions,^{23,24} polymorphic transformations,^{25,26} and very often amorphization.²⁷ Several binary, ternary, quaternary, and quinary chalcogenide compounds easily form on high energy grinding.²⁸ Numerous examples thereof exist (see the Zn-S , Se-S ; Li-Si-S , Li-P-S ; Li-Si-N-S ; and Li-P-Si-N-S systems).^{29–34}

In the $\text{A}_2^+\text{M}^{2+}\text{SnS}_4$ family of compounds, more than forty compounds were reported so far. None of them contains calcium and only $\text{Na}_2\text{MnSnS}_4$ crystallizes in the rocksalt-type structure.³⁵ Therefore, in the present work we report the mechanochemical synthesis of $\text{Na}_2\text{CaSnS}_4$, which is the second member of this family that crystallizes with a rocksalt-type structure. The crystal structure was determined from X-ray powder diffraction data. The average composition was confirmed by EDX and the ionic conductivity was measured by electrochemical impedance spectroscopy. The crystallographic data of all the $\text{A}_2^+\text{M}^{2+}\text{SnS}_4$ compounds were also reviewed.

2. Experimental

2.1. Synthesis

The $\text{Na}_2\text{CaSnS}_4$ sample was prepared by the mechanochemical synthesis route from a stoichiometric mixture of Na_2S (>99.1%, Nagao, Japan), CaS (99.95%, Kishida), and SnS_2 (>99.5%, Mitsubishi Chem.). As for $\text{Na}_2\text{MnSnS}_4$,³⁵ the starting materials (0.5 g in total) were mixed in an agate mortar in a dry Ar glove box. The

Department of Applied Chemistry, Graduate School of Engineering, Osaka Metropolitan University, 1-1 Gakuen-cho, Naka-ku, Sakai, Osaka, 599-8531, Japan.
E-mail: benyahia_hamdi@omu.ac.jp; akitoshihayashi@omu.ac.jp; Tel: +81-72-254-9334

† Electronic supplementary information (ESI) available: Fig. S1 and EDX mapping images of $\text{Na}_2\text{CaSnS}_4$. See DOI: <https://doi.org/10.1039/d4mr00028e>



mixtures were placed in 45 mL zirconia milling pots with 90 g of zirconia balls of 4 mm diameter and mechanically milled using a planetary ball mill apparatus (Pulverisette 7, Fritsch). The rotational speed and milling time were set at 500 rpm and 48 h, respectively without breaks. The obtained dark green powder is hygroscopic.

2.2. Electron microprobe analyses

Semiquantitative EDX analyses of the green powder were carried out on several particles with a JSM-6610A (JEOL) scanning electron microscope (SEM). The experimentally observed Na/Ca/Sn/S atomic ratios were close to 2 : 1 : 1 : 4 as expected for $\text{Na}_2\text{CaSnS}_4$.

2.3. X-ray powder diffraction measurements

XRPD patterns were measured with a Rigaku Smartlab diffractometer using Bragg-Brentano geometry with Cu-K_α radiations. The X-ray data were collected in the 2θ range from 5–80° with a step of 0.01°. The X-ray diffraction data were refined by a Le Bail profile analysis using the Jana2006 program package.³⁶ Since the powder contains an amorphous component, the background was estimated manually, and the peak shapes were described by a pseudo-Voigt function varying four profile coefficients.

Table 1 Crystallographic data and structure refinement for $\text{Na}_2\text{CaSnS}_4$

Crystal data	
Chemical formula	$\text{Na}_2\text{CaSnS}_4$
M_r	333
Crystal system	Cubic
Space group	$Fm\bar{3}m$
Temperature (K)	293
a (Å)	5.6842 (3)
V (Å ³)	183.66 (2)
Z	1
Radiation type	Cu-K_α

Data collection

Diffractometer	Rigaku smartlab
Data collection mode	Bragg Brentano
2θ values (°)	$2\theta_{\min} = 10$ $2\theta_{\max} = 110$ $2\theta_{\text{step}} = 0.01$

Refinement

R factors and goodness of fit	$R_p = 0.013$ $R_{wp} = 0.017$ $R_{\text{exp}} = 0.011$ $R(F) = 0.033$ $R_B = 0.032$ $\chi^2 = 2.190$
No. of parameters	9

2.4. Electrochemical impedance spectroscopy (EIS)

The $\text{Na}_2\text{CaSnS}_4$ sample was characterized by EIS. The powder sample was pelletized at 360 MPa by uniaxial pressing. Gold electrodes were deposited on each face of the pellet using a sputtering apparatus (Quick Coater SC-701MKII Advance; Sanyu Electron Corp.) in an Ar-filled glove box. The conductivity of the sample was then measured on this pellet by an alternating current (AC) impedance technique using an impedance analyzer (SI-1260; Solartron, Metrology, UK) in the frequency range 1.0×10^7 –0.1 Hz and at an applied voltage of 50 mV.

3. Results and discussion

3.1. Structure refinement

The search and match procedure using the ICDD database revealed that the XRPD pattern of the milled $\text{Na}_2\text{CaSnS}_4$ sample was very similar to that of $\text{NaCl}_{0.8}\text{Br}_{0.2}$. The latter crystallizes in the rock salt NaCl-type structure (S. G. $Fm\bar{3}m$). Consequently, a full pattern matching was performed which led to the cell parameters $a = 5.6842$ (3) Å and $V = 183.66$ (2) Å³. For the Rietveld refinement, the cations Na^+ , Ca^{2+} , and Sn^{4+} were set at the 4b Wyck. position (1/2, 1/2, 1/2) and the anions were set at the 4a Wyck. position (0, 0, 0). Restrictions on the occupancies and displacement parameters of Na1, Ca1, and Sn1 were applied. The final residual factors and the refined atomic positions are given in Tables 1 and 2, respectively. Fig. 1 shows an excellent agreement between the experimental and

Table 2 Atomic position and equivalent isotopic displacement parameters for $\text{Na}_2\text{CaSnS}_4$

Atom	Wyck.	Occ.	x	y	z	U_{iso} (Å ²)
Na1	4b	0.5	1/2	1/2	1/2	0.0605(4)
Ca1	4b	0.25	1/2	1/2	1/2	0.0605(4)
Sn1	4b	0.25	1/2	1/2	1/2	0.0605(4)
S1	4a	1	0	0	0	0.0555(6)

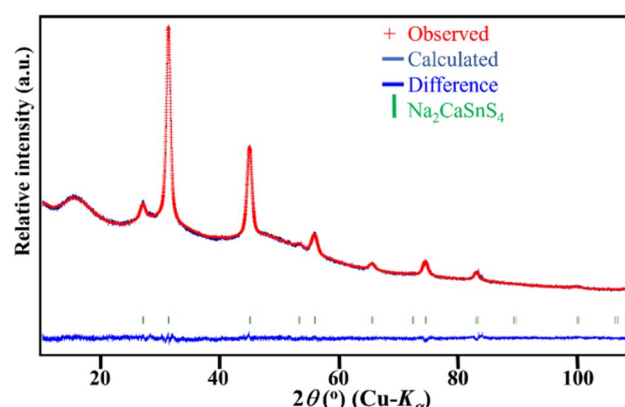


Fig. 1 Observed (cross), calculated (solid line) and difference (bottom) XRPD patterns (Cu-K_α radiation) for $\text{Na}_2\text{CaSnS}_4$.



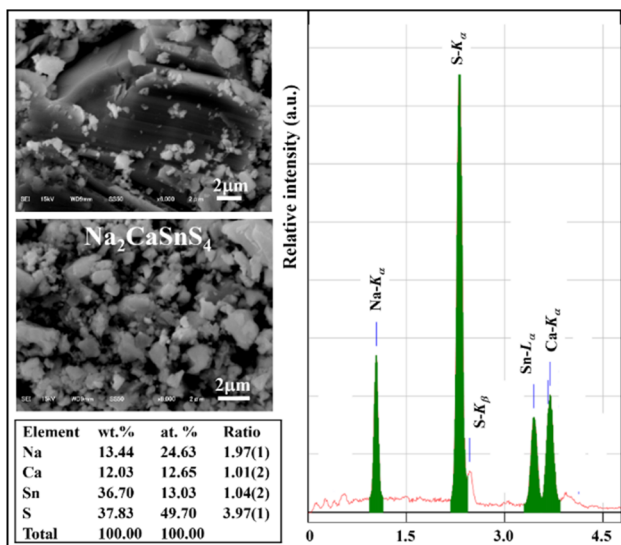


Fig. 2 EDX analysis and SEM micrographs of the milled $\text{Na}_2\text{CaSnS}_4$ sample.

calculated patterns. Furthermore, the Na/Ca/Sn/S atomic ratios of 2 : 1 : 1 : 4 were confirmed by EDX analyses (Fig. 2). Furthermore, the EDX mapping images showed a homogeneous elemental distribution (Fig. S1†).

3.2. Crystal structure of $\text{Na}_2\text{CaSnS}_4$

The title compound $\text{Na}_2\text{CaSnS}_4$ is isostructural to $\text{Ag}_2\text{Sn}^{\text{II}}\text{Sn}^{\text{IV}}\text{S}_4$ (AgSnS_2) which crystallizes in the rock salt-type structure. The crystal structure is depicted in Fig. 3. The sulfur atoms form a cubic close packing with ABC-type arrangement. The statistically disordered sodium, calcium, and tin atoms occupy the octahedral interstices. The Na–S and Ca–S distances of 2.8421(3) Å are in good agreement with 2.86 Å and 2.84 Å, values estimated from the effective ionic radii of the six-coordinated Na^+ , Ca^{2+} , and S^{2-} .⁷⁴ However, the Sn–S distance of 2.8421(3) Å is too large when compared to the 2.53 Å value estimated from the effective ionic radii of the six-coordinated Sn^{4+} and S^{2-} . It should be mentioned that for octahedrally coordinated Sn in SnS_2 ⁷⁵ and Cu_4SnS_6 ,⁷⁶ the Sn–S distances are 2.631 Å and 2.595 Å, respectively. The bond valence sums (BVSs) of 1.17, 2.08, and 1.82 for Na^+ , Ca^{2+} , and Sn^{4+} , respectively confirm that Sn^{4+} is strongly under bonded.⁷⁷

The crystallographic data of all the A_2MSnS_4 compounds are reported in Table 3. Only $\text{Na}_2\text{CaSnS}_4$ and $\text{Ag}_2\text{Sn}^{\text{II}}\text{Sn}^{\text{IV}}\text{S}_4$ crystallize in the rock salt-type structure. Furthermore, in the Na_2MSnS_4 series only 4 compounds are known (M = Mg, Zn, Cd, and Sn). A careful examination of their crystal structures indicated that in the phases with Zn^{2+} or Cd^{2+} the cations are tetrahedrally coordinated, whereas in the phases with Mg^{2+} or Sn^{2+} the cations are octahedrally coordinated. Moreover, a group-subgroup relationship exists between $\text{R}\bar{3}m$ and $\text{Fm}\bar{3}m$.

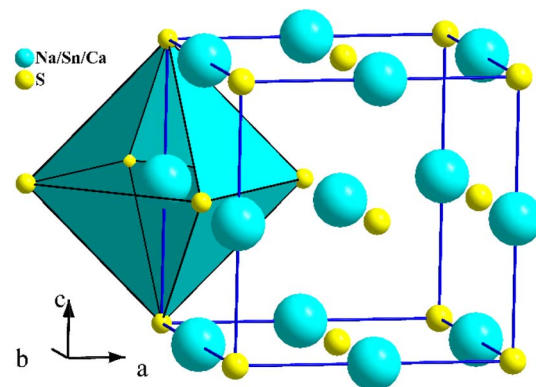


Fig. 3 Crystal structure of $\text{Na}_2\text{CaSnS}_4$.

which suggests the existence of a structural relationship between these phases. Indeed, Heppke & Lerch confirmed that the $\text{Na}_2\text{MgSnS}_4$ ($\text{NaMg}_{1/2}\text{Sn}_{1/2}\text{S}_2$; $hR4$, $\text{R}\bar{3}m$) structure is derived from the NaCl-type structure.⁶⁵ In this structure, the sodium atom occupies the 3b Wyck. position at (0, 0, 1/2) whereas the Mg and Sn are statistically disordered over the 3a Wyck. position at (0, 0, 0). Since in the rock salt structure all cations are disordered over a unique crystallographic site, it is concluded that the change in the crystal structure from the rocksalt-type ($cF8$, $\text{Fm}\bar{3}m$) to the layered-type ($hR4$, $\text{R}\bar{3}m$) is mainly due to the partial ordering of the cations, which is driven by the difference in the size of the cations and the synthesis conditions. Such a phase transition from $\text{Fm}\bar{3}m$ to $\text{R}\bar{3}m$ was observed in many compounds prepared by mechanochemical synthesis and subjected to heat treatments (*i.e.* LiVO_2 , Na_2TiS_3 , and $\text{Na}_2\text{MnSnS}_4$);^{35,78,79} however it was not observed in $\text{Na}_2\text{CaSnS}_4$ which decomposed on heating.

3.3. Ionic conductivity of $\text{Na}_2\text{CaSnS}_4$

AC impedance measurements were performed on a powder compacted pellet of $\text{Na}_2\text{CaSnS}_4$. The Nyquist plot, which consists of a semicircle in the high-frequency region and a spike in the low-frequency region, is depicted in Fig. 4a. The profile indicates that the sample is a typical ionic conductor, and the total resistance of the sample, including the bulk and grain boundary resistances, was used to determine its conductivity. Fig. 4b shows the temperature dependence of the conductivities of $\text{Na}_2\text{CaSnS}_4$. The ionic conductivity of $4.2 \times 10^{-8} \text{ S cm}^{-1}$ ($E_a = 0.6 \text{ eV}$) at 33 °C is much lower than that of the cubic Na_3PS_4 compound ($2 \times 10^{-4} \text{ S cm}^{-1}$ at RT).¹⁴ Although both compounds crystallize in the cubic system and have similar chemical compositions (M_4S_4 with M = Na, Ca, Sn, P), there is a large difference between the ionic conductivities. This is mainly due to the difference in the crystal structures. It seems that the Ca/Sn/Na disorder within the rock salt structure hinders the Na diffusion, whereas the order of Na and P within Na_3PS_4 enables fast Na diffusion. In the future, the synthesis of cation deficient rock salt-type compounds will be performed to



Table 3 Crystallographic data of the $A_2^+M^{2+}SnS_4$ compounds ($A^+ = Li, Na, K, Rb, Cu, Ag, and Tl; M^{2+} = Mg, Mn, Fe, Co, Zn, Cd, Sn, Sr, Ba, Eu, and Hg$)

S. G.	Compound	a (Å)	b (Å)	c (Å)	α (°)	β (°)	γ (°)	V (Å ³)	Ref.
<i>Pn</i>	Li ₂ MnSnS ₄	6.4143(6)	6.8475(6)	8.0078(7)	90	89.980(6)	90	351.71	37
<i>Pna2</i> ₁	Li ₂ MnSnS ₄	13.7036(3)	8.0023(2)	6.4155(2)	90	90	90	703.52	37
<i>Pn</i>	Li ₂ FeSnS ₄	6.3727(3)	6.7776(3)	7.9113(4)	90	90.207(3)	90	341.70	38
<i>Pn</i>	Li ₂ CoSnS ₄	6.3432(2)	6.7184(2)	7.9404(3)	90	89.988(2)	90	338.38	39
<i>Pn</i>	Li ₂ ZnSnS ₄	6.3728(13)	6.7286(13)	7.9621(16)	90	90(3)	90	341.42	40
<i>Pmmn</i>	Li ₂ CdSnS ₄	7.9654(15)	6.4917(15)	6.9685(12)	90	90	90	360.33	41
<i>Pmn2</i> ₁	Li ₂ CdSnS ₄	7.9555(3)	6.9684(3)	6.4886(3)	90	90	90	359.71	42
<i>P3m</i> ₁	Li ₂ Sn ^{II} Sn ^{IV} S ₄	3.67	3.67	7.9	90	90	120	92.15	30
<i>R3m</i>	Li ₂ Sn ^{II} Sn ^{IV} S ₄	3.741(1)	3.741(1)	23.89(10)	90	90	120	289.39	43
<i>Pmn2</i> ₁	Li ₂ HgSnS ₄	7.9400(17)	6.9310(15)	6.5122(14)	90	90	90	358.38	44
<i>I</i> ₄ <i>2m</i>	Cu ₂ MnSnS ₄	5.49	5.49	10.72	90	90	90	323.10	45
<i>I</i> ₄ <i>2m</i>	Cu ₂ FeSnS ₄	5.47	5.47	10.747	90	90	90	321.56	46
<i>P</i> ₄	Cu ₂ FeSnS ₄	5.414(3)	5.414(3)	5.414(3)	90	90	90	158.69	47
<i>I</i> ₄ <i>2m</i>	Cu ₂ CoSnS ₄	5.402	5.402	10.805	90	90	90	315.31	48
<i>I</i> ₄ <i>2m</i>	Cu ₂ ZnSnS ₄	5.4332(2)	5.4332(2)	10.8402(6)	90	90	90	320.00	49
<i>I</i> ₄	Cu ₂ ZnSnS ₄	5.4335(3)	5.4335(3)	10.8429(10)	90	90	90	320.11	50
<i>I</i> ₄ <i>2m</i>	Cu ₂ ZnSnS ₄	5.436	5.436	10.85	90	90	90	320.62	51
<i>Pmn2</i> ₁	Cu ₂ ZnSnS ₄	7.5385	6.4304	6.2038	90	90	90	300.73	52
<i>I</i> ₄ <i>2m</i>	Cu ₂ CdSnS ₄	5.582	5.582	10.86	90	90	90	338.38	51
<i>P</i> ₃ ₁	Cu ₂ SrSnS ₄	6.29	6.29	15.57(8)	90	90	120	533.48	53
<i>P</i> ₃ ₂₁	Cu ₂ SrSnS ₄	6.29	6.29	15.57(8)	90	90	120	533.48	54
<i>Ama</i> ₂	Cu ₂ SrSnS ₄	10.514(3)	10.456(3)	6.425(2)	90	90	90	706.32	55
<i>P</i> ₃ ₁	Cu ₂ BaSnS ₄	6.367	6.367	15.833	90	90	120	555.86	56
<i>P</i> ₃ ₂₁	Cu ₂ BaSnS ₄	6.3711(3)	6.3711(3)	15.8425(12)	90	90	120	556.90	57
<i>Ama</i> ₂	Cu ₂ EuSnS ₄	10.47930(10)	10.3610(2)	6.40150(10)	90	90	90	695.05	58
<i>I</i> ₄ <i>2m</i>	Cu ₂ HgSnS ₄	5.566	5.566	10.88	90	90	90	337.07	51
<i>P</i> _c	Ag ₂ MnSnS ₄	6.6510(10)	6.9430(10)	10.536(2)	90	129.145(3)	90	377.32	59
<i>I</i> ₄ <i>2m</i>	Ag ₂ FeSnS ₄	5.74(3)	5.74(3)	10.96(5)	90	90	90	361.11	60
<i>I</i> ₄ <i>2m</i>	Ag ₂ ZnSnS ₄	5.786(4)	5.786(4)	10.829(6)	90	90	90	362.53	61
<i>Pn</i>	Ag ₂ CdSnS ₄	6.7036(2)	7.0375(3)	8.2166(3)	90	901.577(9)	90	387.63	62
<i>Pmn2</i> ₁	Ag ₂ CdSnS ₄	8.2137(4)	7.0403(4)	6.7033(2)	90	90	90	387.63	62
<i>Fm</i> ₃ <i>m</i>	Ag ₂ Sn ^{II} Sn ^{IV} S ₄	5.506(2)	5.506(2)	5.506(2)	90	90	90	166.92	63
<i>I</i> ₂ ₂₂	Ag ₂ BaSnS ₄	7.127(3)	8.117(3)	6.854(3)	90	90	90	396.50	64
<i>R</i> ₃ <i>m</i>	Na ₂ MgSnS ₄	3.74963(11)	3.74963(11)	19.9130(6)	90	90	120	242.45	65
<i>Fm</i> ₃ <i>m</i>	Na ₂ CaSnS ₄	5.6842(3)	5.6842(3)	5.6842(3)	90	90	90	183.66	^a
<i>Fm</i> ₃ <i>m</i>	Na ₂ MnSnS ₄	5.4368(2)	5.4368(2)	5.4368(2)	90	90	90	160.71	35
<i>R</i> ₃ <i>m</i>	Na ₂ MnSnS ₄	3.7523(4)	3.7523(4)	19.883(2)	90	90	120	242.44	35
<i>I</i> ₄	Na ₂ ZnSnS ₄	6.4835(6)	6.4835(6)	9.1337(10)	90	90	90	383.94	66
<i>C</i> ₂	Na ₂ ZnSnS ₄	9.1749(6)	9.1325(4)	6.4873(5)	90	134.999(4)	90	384.37	67
<i>I</i> ₄ <i>2m</i>	Na ₂ ZnSnS ₄	6.4789(15)	6.4789(15)	9.121(2)	90	90	90	382.86	67
<i>C</i> ₂	Na ₂ CdSnS ₄	9.282(1)	9.421(3)	6.593(9)	90	134.83(9)	90	408.88	68
<i>R</i> ₃ <i>m</i>	Na ₂ Sn ^{II} Sn ^{IV} S ₄	3.69	3.69	25.54	90	90	120	301.16	69
<i>C</i> ₂ / <i>c</i>	K ₂ CdSnS ₄	11.021(5)	11.030(5)	15.151(10)	90	100.416(12)	90	1811.42	70
<i>R</i> ₃	K ₂ Sn ^{II} Sn ^{IV} S ₄	3.67	3.67	25.61	90	90	120	298.73	69
<i>R</i> ₃	Rb ₂ Sn ^{II} Sn ^{IV} S ₄	3.76	3.76	24.33	90	90	120	297.88	69
<i>P</i> ₂ ₁ ₂ ₂	Au ₂ BaSnS ₄	10.982(4)	11.093(4)	6.652(4)	90	90	90	810.37	71
<i>C</i> ₂₂₂ ₁	Au ₂ BaSnS ₄	6.6387(3)	11.0605(7)	10.9676(6)	90	90	90	805.32	72
<i>I</i> ₄ <i>2m</i>	Tl ₂ HgSnS ₄	7.8571(6)	7.8571(6)	6.6989(7)	90	90	90	413.5(1)	73

^a This work.

enhance the sodium diffusion as it was done with the rock salt compound Ag_{3.8}Sn₃S₈.⁸⁰ It should be noted that the relative density of the pellet used for EIS measurements was only 72%. This value could not be improved neither by applying higher pressures nor by sintering the pellets at high temperatures.

Indeed, our prepared sample is metastable. It is a composite material formed of a crystalline phase (rocksalt-type) and an amorphous phase (see in Fig. 1 the hollow feature at low angles).



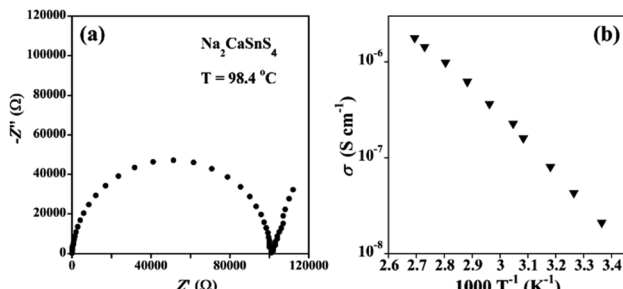


Fig. 4 (a) Typical impedance spectrum acquired at 98.4 °C for the $\text{Na}_2\text{CaSnS}_4$ sample and (b) the temperature dependence of the conductivities.

4. Conclusions

The chalcogenide family of compounds A_2BCD_4 (A^+ = monovalent cation, B^{2+} = divalent cation, C^{4+} = tetravalent cation, and D^{2-} = chalcogen) contains at least 150 members. In this work we demonstrated that the facile mechanochemical synthesis route enables the synthesis of the new member $\text{Na}_2\text{CaSnS}_4$, which is the first quaternary compound of this family that contains calcium and the second to crystallize with a rock salt-type structure. Its ionic conductivity is relatively low when compared with other sulfide ionic conductors such as Na_3PS_4 . Therefore, it would be necessary to prepare other cation deficient phases to enhance the ionic conductivity. This will be conducted in the near future.

Data availability

Our data will be available on request.

Author contributions

H. Ben Yahia designed and performed the experiments and wrote the manuscript and A. Sakuda and A. Hayashi secured the research funds and revised the manuscript.

Conflicts of interest

There are no conflicts to declare.

Acknowledgements

This work was supported by MEXT/JSPS KAKENHI Grant Numbers JP19H05812, JP21H04625 and JP23H04633 and the MEXT program: Data Creation and Utilization-Type Material Research and Development Project Grant Number JPMXP1122712807. We are grateful to Dr Furukawa for his support with EDX analyses and to the reviewers for providing valuable feedback and constructive criticism on this research paper.

References

- 1 S. Mulmi and V. Thangadurai, in *Solid Electrolytes for Advanced Applications*, Springer International Publishing, Cham, 2019, pp. 3–24.
- 2 H.-L. Yang, B.-W. Zhang, K. Konstantinov, Y.-X. Wang, H.-K. Liu and S.-X. Dou, *Adv. Energy Sustainability Res.*, 2021, **2**, 2000057.
- 3 M. Wolf, *Solid State Ionics*, 1984, **13**, 33–38.
- 4 J. B. Goodenough, H. Y.-P. Hong and J. A. Kafalas, *Mater. Res. Bull.*, 1976, **11**, 203–220.
- 5 M. A. Evstigneeva, V. B. Nalbandyan, A. A. Petrenko, B. S. Medvedev and A. A. Kataev, *Chem. Mater.*, 2011, **23**(5), 1174–1181.
- 6 H. Ben Yahia, K. Motohashi, A. Sakuda and A. Hayashi, *Inorg. Chem.*, 2023, **62**(26), 10440–10449.
- 7 K. Motohashi, A. Nasu, T. Kimura, C. Hotehama, A. Sakuda, M. Tatsumisago and A. Hayashi, *Electrochemistry*, 2022, **90**, 22–00037.
- 8 K. Denoue, D. Le Coq, C. Calers, A. Gautier, L. Verger and L. Calvez, *Mater. Res. Bull.*, 2021, **142**, 111423.
- 9 S. Balijapelly, P. Sandineni, A. Adhikary, N. N. Gerasimchuk, A. V. Chernatynskiy and A. Choudhury, *Dalton Trans.*, 2021, **50**, 7372–7379.
- 10 S. Harm, A.-K. Hatz, C. Schneider, C. Hoefer, C. Hoch and B. v. Lotsch, *Front. Chem.*, 2020, **8**, 90.
- 11 L. Gao, G. Bian, Y. Yang, B. Zhang, X. Wu and K. Wu, *New J. Chem.*, 2021, **45**, 12362–12366.
- 12 H. Ben Yahia, K. Motohashi, S. Mori, A. Sakuda and A. Hayashi, *J. Alloys Compd.*, 2023, **960**, 170600.
- 13 F. Tsuji, A. Nasu, C. Hotehama, A. Sakuda, M. Tatsumisago and A. Hayashi, *Mater. Adv.*, 2021, **2**, 1676–1682.
- 14 A. Hayashi, K. Noi, A. Sakuda and M. Tatsumisago, *Nat. Commun.*, 2012, **3**, 856.
- 15 A. Banerjee, K. H. Park, J. W. Heo, Y. J. Nam, C. K. Moon, S. M. Oh, S.-T. Hong and Y. S. Jung, *Angew. Chem., Int. Ed.*, 2016, **55**, 9634–9638.
- 16 Z. Yu, S. Shang, J. Seo, D. Wang, X. Luo, Q. Huang, S. Chen, J. Lu, X. Li, Z. Liu and D. Wang, *Adv. Mater.*, 2017, **29**, 1605561.
- 17 Q. Zhu, J. Wang, X. Liu, N. Ebejer, D. Rambabu and A. Vlad, *Angew. Chem., Int. Ed.*, 2020, **59**, 16579–16586.
- 18 S. Yubuchi, A. Ito, N. Masuzawa, A. Sakuda, A. Hayashi and M. Tatsumisago, *J. Mater. Chem. A*, 2020, **8**, 1947–1954.
- 19 W. S. Tang, K. Yoshida, A. V. Solonin, R. V. Skoryunov, O. A. Babanova, A. V. Skripov, M. Dimitrievska, V. Stavila, S. Orimo and T. J. Urdovic, *ACS Energy Lett.*, 2016, **1**, 659–664.
- 20 Y. Sadikin, M. Brighi, P. Schouwink and R. Černý, *Adv. Energy Mater.*, 2015, **5**, 1501016.
- 21 F. Murgia, M. Brighi and R. Černý, *Electrochim. Commun.*, 2019, **106**, 106534.
- 22 A. Hayashi, N. Masuzawa, S. Yubuchi, F. Tsuji, C. Hotehama, A. Sakuda and M. Tatsumisago, *Nat. Commun.*, 2019, **10**, 5266.
- 23 L. Takacs, *J. Therm. Anal. Calorim.*, 2007, **90**, 81–84.
- 24 Q. Zhang and F. Saito, *Adv. Powder Technol.*, 2012, **23**, 523–531.

25 M. A. Malagutti, V. Z. C. Paes, J. Geshev and C. E. M. de Campos, *RSC Adv.*, 2022, **12**, 33488–33500.

26 M. Senna, *Crystal*, 1985, **20**, 209–217.

27 A. W. Weeber and H. Bakker, *Phys. B*, 1988, **153**, 93–135.

28 P. Baláž, M. Baláž, M. Achimovičová, Z. Bujňáková and E. Dutková, *J. Mater. Sci.*, 2017, **52**, 11851–11890.

29 P. Baláž, M. Bálintová, Z. Bastl, J. Briančin and V. Šepelák, *Solid State Ionics*, 1997, **101–103**, 45–51.

30 T. Fukunaga, S. Kajikawa, Y. Hokari and U. Mizutani, *J. Non-Cryst. Solids.*, 1998, **232–234**, 465–469.

31 H. Yamashita, A. Hayashi, H. Morimoto, M. Tatsumisago, T. Minami and Y. Miura, *J. Am. Ceram. Soc.*, 2000, **103**, 973–978.

32 A. Hayashi, S. Hama, H. Morimoto, M. Tatsumisago and T. Minami, *J. Am. Ceram. Soc.*, 2001, **84**, 477–479.

33 K. Iio, A. Hayashi, H. Morimoto, M. Tatsumisago and T. Minami, *Chem. Mater.*, 2002, **14**, 2444–2449.

34 A. Fukushima, A. Hayashi, H. Yamamura and M. Tatsumisago, *Solid State Ionics*, 2017, **304**, 85–89.

35 H. Ben Yahia, S. Mori, A. Sakuda and A. Hayashi, *J. Solid State Chem.*, 2024, **338**, 124891.

36 V. Petříček, M. Dušek and L. Palatinus, *Z. Kristallogr.–Cryst. Mater.*, 2014, **229**, 345–352.

37 K. P. Devlin, A. J. Glaid, J. A. Brant, J.-H. Zhang, M. N. Srnec, D. J. Clark, Y. Soo Kim, J. I. Jang, K. R. Daley, M. A. Moreau, J. D. Madura and J. A. Aitken, *J. Solid State Chem.*, 2015, **231**, 256–266.

38 C. D. Brunetta, J. A. Brant, K. A. Rosmus, K. M. Henline, E. Karey, J. H. MacNeil and J. A. Aitken, *J. Alloys Compd.*, 2013, **574**, 495–503.

39 J. A. Brant, D. J. Clark, Y. S. Kim, J. I. Jang, A. Weiland and J. A. Aitken, *Inorg. Chem.*, 2015, **54**, 2809–2819.

40 J. W. Lekse, B. M. Leverett, C. H. Lake and J. A. Aitken, *J. Solid State Chem.*, 2008, **181**, 3217–3222.

41 M. S. Devi and K. Vidyasagar, *J. Chem. Soc., Dalton Trans.*, 2002, 2092–2096.

42 J. W. Lekse, M. A. Moreau, K. L. McNerny, J. Yeon, P. S. Halasyamani and J. A. Aitken, *Inorg. Chem.*, 2009, **48**, 7516–7518.

43 A. le Blanc, M. Danot and J. Rouxel, *Bull. Soc. Chim. Fr.*, 1969, **1**, 87–90.

44 K. Wu and S. Pan, *Crystals*, 2017, **7**, 107.

45 J. Allemand and M. Wintenberger, *Bull. Soc. Fr. Mineral. Cristallogr.*, 1970, **93**, 14–17.

46 L. O. Brockway, *Z. Kristallogr.*, 1934, **89**, 434–441.

47 J. Llanos, M. Tapia, C. Mujica, J. Oró-Sole and P. Gómez-Romero, *Bol. Soc. Chil. Quím.*, 2000, **45**, 605–609.

48 W. Schäfer and R. Nitsche, *Mater. Res. Bull.*, 1974, **9**, 645–654.

49 M. Hamdi, A. Lafond, C. Guillot-Deudon, F. Hlel, M. Gargouri and S. Jobic, *J. Solid State Chem.*, 2014, **220**, 232–237.

50 A. V. Chichagov, Eu. G. Osadchii and Z. V. Usyakovskaya, *Neues Jahrbuch fuer Mineralogie, Abhandlungen*, 1986, **155**, 15–22.

51 H. Hahn and H. Schulze, *Sci. Nat.*, 1965, **52**, 426.

52 H. Jiang, P. Dai, Z. Feng, W. Fan and J. Zhan, *J. Mater. Chem.*, 2012, **22**, 7502.

53 C. L. Teske, *Z. Anorg. Allg. Chem.*, 1976, **419**, 67–76.

54 G. L. Schimek, W. T. Pennington, P. T. Wood and J. W. Kolis, *J. Solid State Chem.*, 1996, **123**, 277–284.

55 Y. Yang, K. Wu, B. Zhang, X. Wu and M.-H. Lee, *Chem. Mater.*, 2020, **32**, 1281–1287.

56 C. L. Teske and O. Vetter, *Z. Anorg. Allg. Chem.*, 1976, **426**, 281–287.

57 Y. Liu, X.-D. Song, R.-C. Zhang, F.-Y. Zhou, J.-W. Zhang, X.-M. Jiang, M. Ji and Y.-L. An, *Inorg. Chem.*, 2019, **58**, 15101–15109.

58 J. A. Aitken, J. W. Lekse, J.-L. Yao and R. Quinones, *J. Solid State Chem.*, 2009, **182**, 141–146.

59 D. Friedrich, S. Greil, T. Block, L. Heletta, R. Pöttgen and A. Pfitzner, *Z. Anorg. Allg. Chem.*, 2018, **644**, 1707–1714.

60 R. Caye, Y. Laurent, P. Picot, R. Pierrot and C. Lévy, *Bull. Soc. Fr. Mineral. Cristallogr.*, 1968, **91**, 383–387.

61 Z. Johan and P. Picot, *Bull. Minéral.*, 1982, **105**, 229–235.

62 E. M. Heppke, S. Berendts and M. Lerch, *Z. Naturforsch. B*, 2020, **75**, 393–402.

63 A. Wold and R. Brec, *Mater. Res. Bull.*, 1976, **11**, 761–765.

64 C. R. L. Teske and O. Vetter, *Z. Anorg. Allg. Chem.*, 1976, **427**, 200–204.

65 E. M. Heppke and M. Lerch, *Z. Naturforsch. B*, 2020, **75**, 721–726.

66 J. He, Y. Guo, W. Huang, X. Zhang, J. Yao, T. Zhai and F. Huang, *Inorg. Chem.*, 2018, **57**, 9918–9924.

67 E. M. Heppke, T. Bredow and M. Lerch, *Z. Anorg. Allg. Chem.*, 2022, **648**, e202200216.

68 M. S. Devi and K. Vidyasagar, *J. Chem. Soc., Dalton Trans.*, 2002, 2092–2096.

69 A. le Blanc and J. Rouxel, *C. R. Séances Acad. Sci., Ser. C*, 1972, **274**, 786–788.

70 M.-H. Baiyin, G. Gang and J.-R.-G. Naren, *Chin. J. Inorg. Chem.*, 2014, **30**, 405–410.

71 C. L. Teske, *Z. Anorg. Allg. Chem.*, 1978, **445**, 193–201.

72 C. L. Teske, H. Terraschke, S. Mangelsen and W. Bensch, *Z. Anorg. Allg. Chem.*, 2020, **646**, 1716–1721.

73 L. Piskach, M. Mozolyuk, A. Fedorchuk, I. Olekseyuk and O. Parasyuk, *Chem. Met. Alloys*, 2017, **10**, 136–141.

74 R. D. Shannon, *Acta Crystallogr., Sect. A*, 1976, **32**, 751–767.

75 J. Kaur, Sunaina, Z. Zaidi and S. Vaidya, *Bull. Mater. Sci.*, 2020, **43**, 298.

76 X.-a Chen, H. Wada and A. Sato, *Mater. Res. Bull.*, 1999, **34**, 239–247.

77 I. D. Brown and D. Altermatt, *Acta Crystallogr., Sect. B*, 1985, **41**, 244–247.

78 A. Nasu, M. Otoyama, A. Sakuda, A. Hayashi and M. Tatsumisago, *J. Ceram. Soc. Jpn.*, 2019, **127**, 514–517.

79 J. Chable, C. Baur, J. H. Chang, S. Wenzel, J. M. García-Lastra and T. Vegge, *J. Phys. Chem. C*, 2020, **124**, 2229–2237.

80 O. Amiel, D. C. Frankel and H. Wada, *J. Solid State Chem.*, 1995, **116**, 409–421.

